On the Bending Analysis of Multi-Cracked Slender Beams with Continuous Height Variations

Matjaž Skrinar[1*], Denis Imamović[1]

Abstract

We studied the implementation of a multi-stepped multi-cracked beam finite element for analysing beams of various heights' variations along the length. The genuine continuous variation of height was modelled by an adequate series of steps and for the cracks, the model of internal hinges endowed with rotational springs was applied. As the increased number of steps simultaneously increases the possibility that the crack location and step location may coincide, the continuous conditions at the steps were rewritten to a more general form in order to cover this combination. The newly presented form is also capable of taking a transverse concentrated force into account. Numerical evaluations were performed for several structures under various loads and the transverse displacements, nodal reactions, and inner forces were studied. The results obtained are positioned side by side with the results from more detailed 2D finite element meshes. The comparisons show excellent matching of the beam's response providing the mesh of steps was dense enough. The examples demonstrate the potential of the present approach proving that the model is suitable for achieving computationally-efficient and truthful analyses.

Keywords

cracked beams with transverse cracks, continuous cross-sections' variations, simplified computational model, finite element method, transverse displacements

1 Introduction

As the cracks are degenerative effects that might severely impact the behaviour of engineering structures, their immediate detection is vitally important for safety reasons. However, the efficiency of structural health monitoring is a combination of accurate data measurements and the versatility of mathematical representation of mechanical behaviour. Although suitable 2D or 3D meshes of finite elements yield the best description of the crack and its surroundings, this approach is advantageous only when all the crack's details are known in advance. Consequently, simplified models are more efficient for inverse problems where none of the potential crack's details (presence, location, intensity) is known.

The appropriate simplified model that has been the subject of numerous researches in the past, is the model provided by Okamura et al. [1]. This model simulates cracks by massless rotational linear springs. Each spring connects those neighbouring non-cracked parts of the beam that are modelled as elastic elements and the linear moment-rotation constitutive law is adopted. Such a mathematical model allows for all the essential data (transverse displacements and inner forces) to be evaluated with adequate accuracy.

Okamura's computational model was effectively implemented in finite element solutions for the computation of transverse displacements. Initially, Gounaris and Dimarogonas [2] presented a numerical procedure for the computation of a beam element with a single transverse crack. Afterwards, closed-form solutions for the static transverse displacements and stiffness matrix of a beam's finite element having an arbitrary number of transverse cracks have been derived at by several authors by implementing different mathematical methods. The Dirac delta function was implemented twice: by Biondi and Caddemi [3] in regard to the rigidity, and by Palmeri and Cicirello [4] in regard to the flexibility. Sequential solutions of coupled differential equations were implemented by Skrinar [5], while Skrinar and Pliberšek [6] implemented the principle of virtual work.

Due to its simplicity (the depth and the location are the only crack's parameters required) the "discrete spring" model has been intensively implemented in vibration analysis of cracked

1 Department of Structural Mechanics
   Faculty of Civil Engineering, Transportation Engineering and Architecture
   University of Maribor
   Smetanova 17, 2000 Maribor, Slovenia
* Corresponding author, email: matjaz.skrinar@um.si

beams (Labib et al. [7], F. Bakhtiari-Nejad et al. [8]). Furthermore, several authors have recently proposed new various approaches for inverse identification of cracks (Labib et al. [9], Khien and Toan [10], Khiem and Tram [11], Sung et al. [12]), while Cao et al. [13], and Gawande and More [14], have also presented some experiments.

While the vast majority of the research is limited to elements with constant cross sections Skrinar [15] presented beam finite element solution (MCSBFE) for bending analysis of stepped-beams and beams with linearly-varying heights. The implementation of the principle of virtual work brought clear recognition of the separate impact of cracks as well as beams' geometries into the response analysis. The stiffness matrix and the load vector are namely governed by four damage coefficients that gather all damage data, and four geometric coefficients that cover the beam's geometric parameters. By deriving at expressions for a beam with a linearly-varying height Skrinar [15] indicated that it is achievable to obtain unique analytical expressions for almost any arbitrary variation of a cross section's height. However, it can be concluded from those expressions that such derivations will lead to very complex forms. Consequently, this indicates that it might be wiser to model numerically not only the cracks but the non-uniform non-cracked parts of the structure as well. This can be achieved rather straightforwardly by implementing an adequately high numbered series of finite steps, for which some fundamental generalised expressions have already been defined. In this way not only the cracks but the rest of the complete structure also (i.e. non-cracked, as well as cracked parts) is adequately modelled by an alternative model. This paper thus studies the implementation of the multi-stepped cracked beam model for various variations of cross-sectional height, simultaneously illustrating the robustness of the numerical simulation.

2 Calculation of stiffness matrix's coefficients

An arbitrary height's variation can be efficiently modelled by a series of steps of piecewise uniform height. The adequateness of such a model, and simultaneously of the results, clearly increases with the number of implemented steps. It was shown (Skrinar, [15]) that an element's stiffness matrix consists of two mutually independent types of coefficients: damage coefficients α and geometric coefficients β. The damage coefficients depend solely on the depths and locations of cracks and are not influenced by the (non-damaged) geometry i.e. number and/or combinations of the steps. Therefore, their evaluation in this paper follows the already presented equations. On the other hand, the geometric coefficients β depend solely on the non-damaged variable geometry of the beam which strongly influences the number of required segments N_s, Fig. 1.

This number tends to be high because the increased number of segments is directly reflected in the better quality of the results. With this in mind, it is probably the most suitable approach to
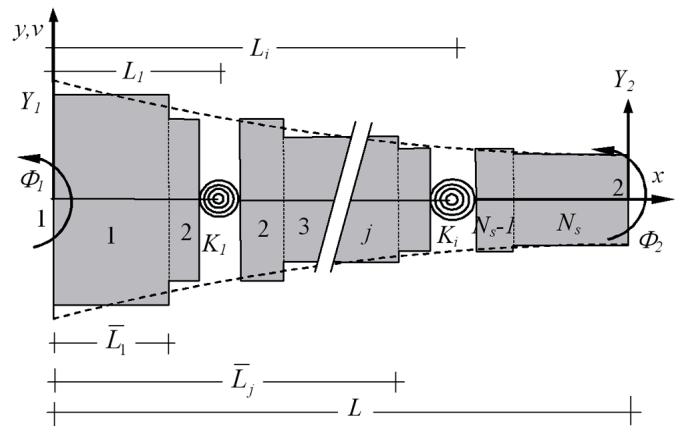

Fig. 1 The model of multi-stepped multi-cracked beam

select steps of equal lengths along the whole element. Although the previously presented equations for geometric coefficients are already fully applicable for their evaluation, a uniform length of steps allows for the coefficients to be written in a form that enables faster computation. By introducing the coefficient (with EI_i being uniform flexural rigidity of the i-th step)

$$\overline{c}_j = \sum_{i=1}^{N_s} \frac{i^j}{EI_i} \qquad j = 0,1,2,3 \tag{1}$$

the geometric coefficients are further given as (i = 1, 2, 3, 4):

$$\beta_i = \left(-\frac{L}{N_s}\right)^i \cdot$$
$$\left(-\frac{\overline{c}_o}{i} + \sum_{k=1}^{3}\left(H[i-k-1]\cdot \overline{c}_k\right) - H[i-3]\cdot\frac{1+i}{2}\cdot\overline{c}_2\right) \tag{2}$$

where ratio L/N_s represents the uniform length of each step and H stands for Heaviside step function of an integer variable.

3 Computation of exact transverse displacements along the finite element

The general mathematical form of the GDE's solution for each elastic segment of a stepped beam is a complete polynomial of the third degree plus an additional term that takes uniform load into account:

$$w_i(x) = a_i + b_i \cdot x + c_i \cdot x^2 + d_i \cdot x^3 + \frac{q^{[4]}(x)}{EI_i} \tag{3}$$

where $q^{[m]}(x)$ denotes the m-th anti-derivative of the transverse continuous load $q(x)$ without a constant of integration, while a_i, b_i, c_i and d_i represent constants of integration. These four unknown coefficients can be determined either from the boundary conditions at the ends of the finite element (for i = 1 or $i = N_s$) or the continuity conditions between two consecutive elastic segments (for $1 < i < N_s$).

In past study, the continuity conditions were derived at for two separated situations: a discrete-step-change of the cross-section, and a crack. Due to the increased number of steps the chances that the location of a crack coincides with the discrete-step-changes of the cross-section, are increasing.

Therefore, the already derived at continuity conditions have to be rewritten in a more general form to also cover this situation. The presented study thus generalises the known expressions and presents those continuity conditions that are also applicable for a crack located at the discrete-step-change of the cross-section. The presented expressions are further expanded to also cover the case when a concentrated transverse force F is applied at the discrete-step-change of the cross-section.

A concentrated transverse load F (positive upward), located at the beginning of the i-th ($i > 1$) discrete-step-change (at distance $\overline{L}_{i-1}$), directly influences the computation of coefficient d_i for this elastic section. The expression that allows for a coefficient to be obtained from the equilibrium of shear forces is:

$$d_i = \frac{d_{i-1} \cdot EI_{i-1} + F}{EI_i}. \tag{4}$$

A concentrated force indirectly (over the coefficient d_i) also impacts evaluation of the remaining coefficients at the i-th segment. In order to operate with a unique expression valid for both situations (regardless of the presence of a concentrated force F), the coefficient c_i is given as:

$$c_i = \frac{c_{i-1} \cdot EI_{i-1} + 3 \cdot (d_{i-1} \cdot EI_{i-1} - d_i \cdot EI_i) \cdot \overline{L}_{i-1}}{EI_i}. \tag{5}$$

It can be easily shown that Eq.(5) which was obtained from the equilibrium of bending moments transforms into an already presented expression when F vanishes.

A crack (with a rotational spring K_r), located at the beginning of the i-th ($i > 1$) discrete-step-change (at distance $\overline{L}_{i-1}$), directly influences the calculation of coefficient b_i for this elastic section. The coefficient b_i obtained from the slope's continuity condition is given as:

$$
\begin{aligned}
b_i = {} & b_{i-1} + 2 \cdot (c_{i-1} - c_i) \cdot \overline{L}_{i-1} + 3 \cdot (d_{i-1} - d_i) \cdot \overline{L}_{i-1}^2 \\
& + \left(\frac{1}{EI_{i-1}} - \frac{1}{EI_i} \right) \cdot q^{[3]}(\overline{L}_{i-1}) \\
& + \frac{2 \cdot c_{i-1} \cdot EI_{i-1}}{K_r} + \frac{6 \cdot d_{i-1} \cdot EI_{i-1} \cdot \overline{L}_{i-1}}{K_r} + \frac{q^{[2]}(\overline{L}_{i-1})}{K_r}.
\end{aligned} \tag{6}
$$

Evidently, for the non-cracked situation (i.e. "simple step") the last three terms of Eq.(6) vanish.

Whilst the crack has no influence on coefficients d_i and c_i, the presence of transverse concentrated force F indirectly influences the b_i coefficient over coefficients d_i and c_i.

A crack indirectly (over the coefficient b_i) also influences the coefficient a_i. A sole expression valid for all situations (with or without the presence of a concentrated force F, non-cracked or cracked), the coefficient a_i is given as:

$$
\begin{aligned}
a_i = {} & a_{i-1} + (b_{i-1} - b_i) \cdot \overline{L}_{i-1} + (c_{i-1} - c_i) \cdot \overline{L}_{i-1}^2 \\
& + (d_{i-1} - d_i) \cdot \overline{L}_{i-1}^3 + \left(\frac{1}{EI_{i-1}} - \frac{1}{EI_i} \right) \cdot q^{[4]}(\overline{L}_{i-1}).
\end{aligned} \tag{7}
$$

Equation (7) has been obtained from the continuity condition for displacement.

The present equations are valid not only when discrete-step change, crack and transverse force F appear simultaneously at a single point of the beam-element, but also if each of these events appears individually.

4 Numerical examples

The concise results from three beam structures differing in cross-sectional variations, boundary conditions, number and locations of the cracks, as well as applied loads, are given below. The transverse displacements along the axis, reactions at the supports, as well as inner forces were evaluated by utilising various discretisations in order to examine the minimum numbers of stepped segments required to achieve the convergence of the results. Transverse displacements and inner forces were obtained in analytical form for each segment.

The quality of the obtained values was (exclusively for verification reasons) confirmed by comparing the obtained results to the results from two alternative computational models for each example considered. In the first additional computational beam-model, the cracks were again modelled by rotational springs but exact description of height variation between the cracks was applied. For this model, coupled governing differential equations (GDEs) were solved providing displacements and rotations as well as shear forces and bending moments as analytical piecewise continuous functions between the nodes and cracks.

The ultimate supplementary model was a 2 D finite element model with a detailed description of the cracks and the correct geometric variations. Displacements and inner forces of this model were obtained only in discrete points.

4.1 Example 1 - cantilever

In the first example, an 8 m long multi-cracked cantilever clamped at the left end and loaded with a vertical concentrated load of 1 kN at the right was analysed, Fig. 2, where the height h followed parabolic distribution given by the polynomial of the second degree:

$h(x) = 0.4 - 0.0625 \cdot x + 0.00390625 \cdot x^2$.

The Young's modulus of the material was $E = 30$ GPa with Poisson's ratio 0.3, whilst the constant width b of the cantilever was 0.25 m. Three cracks were introduced, located at distances of 0.5 m, 3 m and 5 m from the left-end. The relative crack-depth was identical for all cracks in order minimise the
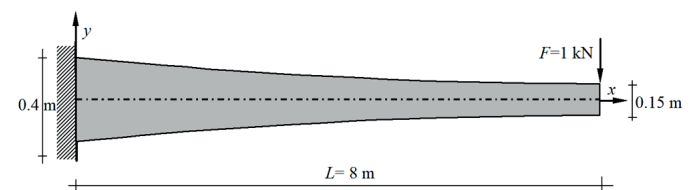

Fig. 2 First example structural setup

influence of the rotational spring-stiffness' definition on the results. The genuine definition given by Okamura was selected from amongst all existing definitions for rotational spring due to the fact that it is the only one that takes Poisson's ratio into account. The selected relative crack-depth was $\delta = 0.5$ as for this value Okamura's definition produces results that have been proved to be in good agreement with those experimentally obtained values, as presented by Vestroni [16]. In the stepped model the real cracks' depths were utilised in evaluations of rotational springs' stiffnesses.

The free end's transverse displacement was evaluated by the principle of virtual work (considering the actual height's variation) for the non-cracked as well as for the cracked case, yielding the values of −14.5632 mm and −20.0712 mm, respectively.

Independent of the number of utilised stepped-segments, the beam FE computational model consisted of a single MCSBFE beam finite-element with just two nodes, thus representing the smallest possible finite-element computational model.

In the first step, several discretisations were studied with various numbers of segments of equal lengths. Their goal was to find out the minimum number of necessary segments for achieving convergence of the results. In these studies, both transverse displacements of the free end obtained by the principle of virtual work were implemented as benchmark values. The results exhibited stable monotonic convergence for both, the non-cracked as well as the cracked case, with similar convergence rates for both cases. It became clearly evident from the results obtained that from the engineering point of view the implementation of more than 80 segments for the cases studied had almost no impact on the accuracy.

The computational model for further comprehensive analysis thus consisted of a single finite element with 80 stepped segments. The model had four degrees of freedom. However, by considering known zero displacement and rotation at the left end of the element the discrete unknowns (vertical displacement v_2 and rotation Φ_2 at the free end) were evaluated from a simple system of two linear equations:

$$\begin{bmatrix} 144535.5 & -376368.2 \\ -376368.2 & 1495545.9 \end{bmatrix} \cdot \begin{Bmatrix} u_2 \\ \Phi_2 \end{Bmatrix} = \begin{Bmatrix} -1000 \\ 0 \end{Bmatrix}.$$

These discrete values further allowed for the computation of nodal vertical reaction force and bending moment of the clamped-end over the element's stiffness matrix. They additionally allowed for the calculation of transverse displacements along the longitudinal axis of the structure.

By implementing the 80 elastic segments model all the cracks' locations coincided with the locations of the discrete height variation. Therefore, solely 80 displacement functions had to be analysed in order to obtain vertical displacement distributions along the structure.

The transverse displacement function's coefficients of the first segment were obtained by exclusively implementing the boundary conditions at the left-end. The remaining 79 functions were afterwards consecutively evaluated by applying the continuity conditions between the corresponding two neighbouring segments. Four boundary conditions at the right-end remained unused and therefore served for verification purposes only.

Due to the rather dense mesh of steps, just discrete values of displacement at the steps' connections would be sufficient for successful displacement graphical presentation. Nevertheless, all four coefficients were evaluated for each segment, which further allowed for the determination of segment's bending moments and shear forces' functions. For example, the last region's function was thus obtained as:

$$w_{80}(x) = -2.0107 \cdot 10^{-2} + 1.0116 \cdot 10^{-2} \cdot x - 1.8959 \cdot 10^{-3} \cdot x^2 + 7.8997 \cdot 10^{-5} \cdot x^3 \quad 7.9\text{m} \le x \le 8\text{m}$$

The transverse displacements of the considered structure's simplified computational model were further analysed by solving a system of four coupled governing differential equations. These were governing equations of the computational model with rotational springs representing cracks and actual description of heights' variations amongst them. The structure considered is statically determinate and the bending-moment's distribution was thus obtainable from the basic equilibrium. Thus, the differential equations were of second-order. This approach allowed for the actual distribution of the simplified model's transverse displacements to be evaluated.

The obtained values from the simplified model were further compared to the results obtained from the more detailed computational model of the considered structure. These results were obtained through a 2D plane elements computational model by implementing a SAP2000 v15.0.0 finite element program. The transverse displacements and reactions were obtained from a computational model consisting of 3,330 2D plane elements with 3,669 joints. In each node, two degrees of freedom were taken into account – vertical and horizontal displacements. Vertical and horizontal displacements of discrete nodal points were obtained by solving approximately 7,300 linear equations.

The results for several significant discrete parameters (vertical reaction V_A and bending moment M_A at the left support, transverse displacements at cracks' locations and at the free end, rotation φ_B at the free end) from all the applied computational models were compared and are summarised in Table 1.

Table 1 Comparisons of the results for the cantilever from three different computational approaches

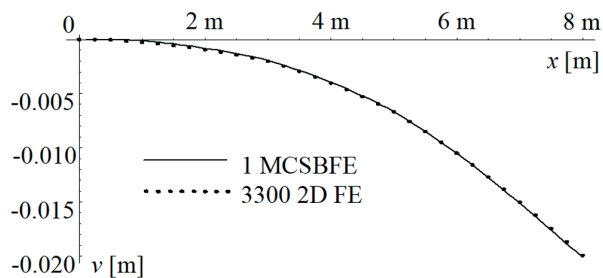| Parameter	1 MCSBFE	4 GDEs	SAP2000
V_A	1000 N	1000 N	1000 N
M_A	8000 Nm	8000 Nm	8000 Nm
v(0.5 m) [mm]	−0.02654	−0.02649	−0.026
v(3 m) [mm]	−1.9973	−1.9969	−2.000
v(5 m) [mm]	−6.6834	−6.6826	−6.675
v(8 m) [mm]	−20.0727	−20.0712	−19.927
φ_B [rad]	-5.0515×10^{-3}	-5.0513×10^{-3}	-5.001×10^{-3}

Fig. 3 Comparison of transverse displacements of cantilever from two applied models

It is evident from the table that multi-stepped approximation of the actual variation of the height yields results that are from the engineering point of view basically identical to the GDE's solutions. It is furthermore evident from the last two columns of the table that simple crack's modelling (in combination with GDEs) offers solutions fully comparable with the more detailed plane finite model.

The table shows that the overall matching of the results between the single MCSBFE element model and 3,000 2D FE model is very good. The average discrepancy of the displacements is slightly smaller than 0.26 %, and the error at maximum displacement's location is around 0.73 %.

The comparison between transverse displacements along the axis obtained by two implemented models is given in Fig. 3, where only very small discrepancies are noticeable.

The obtained displacements' functions from the single MCSBFE model were further implemented in the derivation of bending moments' functions. The obtained distribution and corresponding values were identical as from basic static equilibrium analysis.

4.2 Example 2 – simply supported beam

In the second example, an 8 m long multi-cracked simply supported beam loaded with a vertical concentrated load of 100 kN at the mid-span was analysed, Fig. 4. For this structure, the height h followed a parabolic distribution of the polynomial of second degree:

$$h(x) = 0.4 - 0.00390625 \cdot x^2.$$

The Young's modulus of the material was $E = 30$ GPa with Poisson's ratio 0.3, whilst the width b of the beam was 0.25 m. Two cracks were introduced, located at distances of 1 m and 4.5 m from the left-end. The relative crack-depth was taken to be $\delta = 0.5$ for both cracks and the genuine definition given by Okamura was used again. The computational model consisted of a single MCSBFE finite-element with just two nodes.
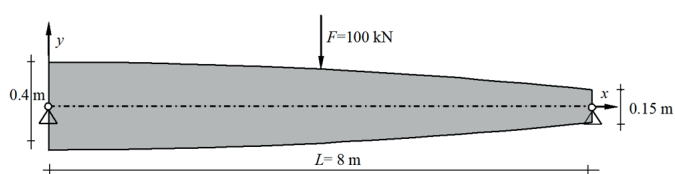

Fig. 4 Second example structural setup

In the first step, the minimum number of required segments of equal lengths was studied to achieve convergence of the results. The transverse displacement of the mid-span served as a reference value. As in the first example, a monotonic convergence of the results was detected. Furthermore, it appeared again that the implementation of more than 80 segments had insignificant any effect on the accuracy. The computational model consisting of a single finite element with four degrees of freedom and 80 stepped segments was thus implemented for further detailed analysis. By considering known displacements at both ends of the element the discrete unknowns (rotations Φ_1 and Φ_2 at both ends) were evaluated from a simple system of two linear equations:

$$\begin{bmatrix} 1400090.1 & 2781012.4 \\ 2781012.4 & 3005494.9 \end{bmatrix} \cdot \begin{Bmatrix} \Phi_1 \\ \Phi_2 \end{Bmatrix} = \begin{Bmatrix} -146778.28 \\ 45735.22 \end{Bmatrix}$$

Implementing the obtained discrete values of both nodals' rotations corresponding nodal vertical reaction forces as well as the distribution of transverse displacements along the longitudinal axis of the structure were further evaluated.

The considered structure was further analysed for verification reasons only. Therefore, transverse displacements were obtained by solving a system of four coupled governing differential equations. In this computational model, an actual description of the heights' variations was considered whilst the cracks were again represented by rotational springs. The bending moment's distribution is obtainable from basic equilibrium (the structure considered is statically determinate) and, consequently, the differential equations were again of second-order. In this way, actual distribution of the simplified model's transverse displacements was evaluated.

In addition, this example was further analysed by implementing a computational model with 3,546 2D plane finite elements. The comparison of transverse displacements along the axis obtained by MCSBFE and 2D plane finite elements model is given in Fig. 5. Only very small discrepancies are noticeable.

Furthermore, the discrete values of some representative quantities (vertical reaction VA and rotation jA at the left support, vertical reaction VB and rotation jB at the right support, transverse displacements at cracks' locations and at the mid-span) are summarised in Table 2.
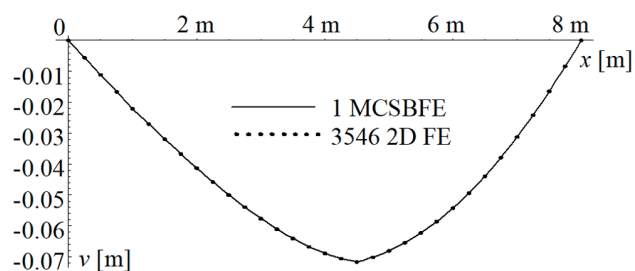

Fig. 5 Comparison of transverse displacements of simply supported beam from two applied models

Table 2 Comparisons of the results for the simply supported beam from three different computational approaches

Parameter	1 MCSBFE	4 GDEs	SAP2000
V_A	50000 N	50000 N	50000 N
φ_A [rad]	-2.2300×10^{-2}	-2.2301×10^{-2}	-2.263×10^{-2}
V_B	50000 N	50000 N	5000 N
φ_B [rad]	3.3562×10^{-2}	3.3568×10^{-2}	3.3779×10^{-2}
$v(1 \text{ m})$	-22.0930 mm	-22.0912 mm	-22.083 mm
$v(4.0 \text{ m})$	-68.8062 mm	-68.7994 mm	-68.713 mm
$v(4.5 \text{ m})$	-71.6253 mm	-71.6180 mm	-71.476 mm

The table shows that the single MCSBFE's values for vertical reactions in the supports are identical to the values from the basic static analysis. Furthermore, it is evident from the table that although the displacements obtained by the multi-stepped finite element are just slightly higher than those from the 2D finite element model, the matching of the results is very good. The discrepancy of the displacements increases from the supports toward the maximum displacement (appearing at the location of the second crack) where it is slightly smaller than 0.21 %.

The obtained displacements' functions from the single MCSBFE model were further implemented for the derivation of bending moments' evaluations. The obtained distribution and corresponding values were identical to the basic static equilibrium analysis.

4.3 Example 3 – propped cantilever

In the third example, a multi-cracked propped cantilever was analysed, Fig. 6. It was loaded by a vertical uniform load of 10 kN/m over the whole length of 10 m.

For this structure the height h was varied from 0.2 m at the mid-span to 0.4 m at both ends following the trigonometric distribution:

$$h(x) = 0.3 + 0.1 \cdot \cos(0.2 \cdot \pi \cdot x).$$

The Young's modulus of the material was $E = 30$ GPa with Poisson's ratio 0.3, whilst the width b of the cantilever was 0.25 m. Three cracks were introduced, located at distances of 2 m, 5 m, and 6 m from the left-end which was clamped. The relative crack-depth was again taken to be $\delta = 0.5$ for all cracks and the genuine definition given by Okamura was implemented again. The computational model consisted of a single presented beam finite-element with just two nodes, thus representing the smallest possible finite-element computational model.
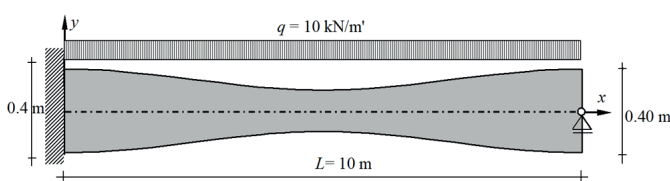
Fig. 6 Third example structural setup

The number of implemented segments of equal lengths was restricted to 100 after conducting a short convergence study with the transverse displacement of the mid-span serving as the point of reference. It should be noted that from the pure engineering point of view just 20 segments would produce almost identical results.

The computational model consisted of a single finite element (with 100 stepped segments) with four degrees of freedom. However, by considering zero rotation at the left-node, as well as zero transverse displacements at both ends, the discrete value of the rotation Φ_2 at the right-node was evaluated from a single linear equation (for $N_s = 100$):

$$7567586.2094 \cdot \Phi_2 = 114943.2665.$$

This single value allowed for the computation of nodal vertical reaction forces and bending moment as well as the distribution of transverse displacements along the longitudinal axis of the structure.

This structure was further analysed by solving the system of four coupled governing differential equations of a computational model with actual descriptions of heights variation' and the cracks represented by rotational springs. In contrast to previous examples, the structure was statically indeterminate and, consequently, the differential equations were of fourth-order. However, when analyzing this structure's GDEs noticeable mathematical limitations appeared. When integrating the bending moments the results for rotations start to appear in the form of a polylogarithmic function which caused integration problems. Therefore, for each of four segments, the exact ratio $1/EI(x)$ was replaced by a Taylor series consisting of up to 12 terms. The average discrepancy for such a description of flexural rigidity against exact values was 0.006 % whilst the maximum discrepancy was slightly below 0.25 %. Such an approach allowed for transverse displacements and inner forces to be further obtained without any mathematical inconveniencies.

In addition, this example was also analysed by implementing a computational model with 7,040 2D plane finite elements. Fig. 7 thus represents the distribution of transverse displacements from all computations.

Furthermore, the discrete values of vertical reaction V_A and bending moment M_A at the left support, vertical reaction V_B and rotation φ_B at the right support, transverse displacements at cracks' locations, location x_{max} and value v_{max} of maximal transverse displacement are summarised in Table 3.
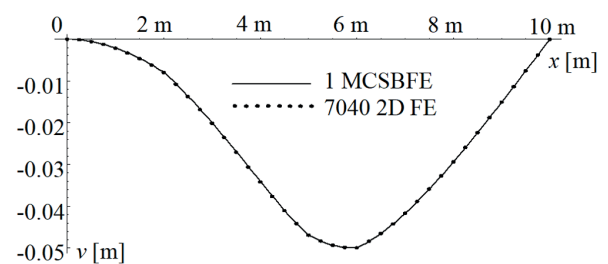
**Fig. 7** Comparison of transverse displacements of propped cantilever from two applied models

Table 3 Comparison of results for the propped cantilever using three different computational models

Parameter	1 MCSBFE	4 GDEs	SAP2000
V_A	68787.91 N	68788.355 N	68674 N
M_A	187879.100	187883.547	186562
V_B	31212.09 N	31211.65 N	31328 N
φ_B [rad]	15.188×10^{-3}	15.1880×10^{-3}	15.439×10^{-3}
$v(2\text{ m})$	−7.8834 mm	−7.8825 mm	−7.96 mm
$v(5\text{ m})$	−46.854 mm	−46.852 mm	−46.868 mm
x_{max}	5.93 m	5.93 m	5.91 m
v_{max}	−49.918 mm	−49.916 mm	−49.882 mm
$v(6\text{ m})$	−49.899 mm	−49.897 mm	−49.867 mm

It is evident from Table 3 that the implementation of 100 steps reflects an obvious agreement of the results. The absolute maximum difference in displacement – appearing at the first crack – is smaller than 1.0 %, whilst the differences at the second and third crack are approximately 0.03 % and 0.06 %, respectively.

For the vertical reactions, the differences were somehow higher. The differences for vertical reactions at the left and right supports were slightly smaller than 0.17 % and 0.37 %, respectively, whilst the difference for bending-moment at the left-support was about 0.7 %.

The obtained displacements' functions from the stepped model were further implemented for the derivation of bending moments' evaluations. Their distribution is given in Fig. 7. As this structure was statically indeterminate and the moments could not be evaluated from a simple static analysis, more attention was paid to their verification. Therefore, the GDEs' solutions were also implemented for the derivations of bending moments. Although four separated displacement functions were required to accurately describe the transverse displacements, all these functions led to a unique function of bending moments. It is evident from Fig. 7 that both approaches based on the simplified model produced the results that match outstandingly. In order to complete this, discrete values of bending moments were also evaluated from a 2D plane finite elements model. The values were obtained by numerically integrating discrete nodal normal stresses in the axial direction. Also, these values exhibit excellent agreement (Fig. 8) with other values thus confirming the quality of the discussed simplified stepped model.
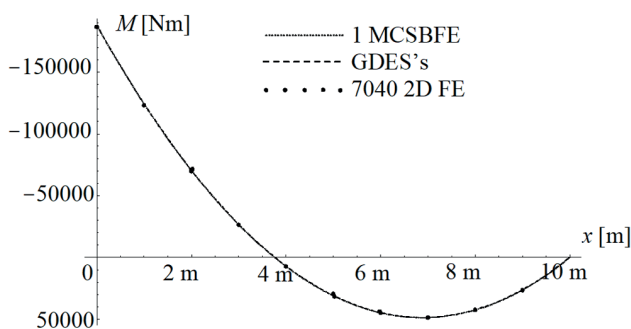
Fig. 8 Distribution of bending moments of the propped cantilever

This example is also instructive from another point of view. In contrast to the first two examples, where GDE's solutions were obtained in a rather simple straight-forward manner, the trigonometric variation of the height caused certain mathematical difficulties. However, it should be noted that, on the other hand, the considered variation in height did not cause any problems within the stepped model as direct integration was not required. Consequently, this example indirectly suggests that the stepped model for the complex heights' variations offers mathematically more stable and straight-forward solutions than GDEs.

5 Conclusions

This paper studied the behaviour of multi-cracked slender beams where their heights varied along the length of the structure. Within the implemented computational model two essential simplifications were taken into account. Firstly, transverse cracks were represented by means of internal hinges endowed by rotational springs, which is the approach that has already been proven to be effective and reliable. Secondly, the genuine continuous heights' variations were replaced by sufficiently larger numbers of finite-length steps. This computational model allows for the stiffness matrix and the load vector to be written in closed-symbolic forms.

As for a computationally efficient modelling of heights' variation, a higher number of segments is required, it is the more suitable (although unnecessary) way to implement steps of equal lengths. Therefore, in order to facilitate computation, the geometric coefficients were revaluated and are presented in an extremely efficient form.

With the increased number of steps, the situation where the discrete change of a segment's height coincides with a crack's location becomes almost unavoidable. Therefore, to also cover this situation the continuity conditions of displacement functions are presented in a more generalised form combining a discrete-step and a crack at a single point. These newly-presented coefficients additionally allow for the concentrated transverse force acting at this point to be taken into analysis. Again, these novel terms are presented in closed-forms that facilitate their implementation.

Three numerical examples differing in geometry, boundary conditions and implemented loads follow the theoretical section. These studies show that the presented expressions produced excellent results that were confirmed independently by more thorough 2D plane models. The examples thus clearly demonstrated that adequate numerical modelling of height's variations by multi-stepped elements is exceptionally effective. Furthermore, the last example even showed that for some complex heights' variations the stepped-model approach solutions can be mathematically more straight-forward than solving the governing differential equations.

Acknowledgement

References

[1] Okamura, H., Liu, H. W., Chu, C-S., Liebowitz, H. "A cracked column under compression". *Engineering Fracture Mechanics*, 1(3), pp. 547–564. 1969.
https://doi.org/10.1016/0013-7944(69)90011-3

[2] Gounaris, G., Dimarogonas, A. "A finite element of a cracked prismatic beam for structural analysis". *Computers and Structures*, 28(3), pp. 309–313. 1988.
https://doi.org/10.1016/0045-7949(88)90070-3

[3] Biondi, B., Caddemi, S. "Euler-Bernoulli beams with multiple singularities in the flexural stiffness". *European Journal of Mechanics - A/Solids*, 26(5), pp. 789–809. 2007.
https://doi.org/10.1016/j.euromechsol.2006.12.005

[4] Palmeri, A., Cicirello, A. "Physically-based Dirac's delta functions in the static analysis of multi-cracked Euler-Bernoulli and Timoshenko beams". *International Journal of Solids and Structures*, 48(14–15), pp. 2184–2195. 2011.
https://doi.org/10.1016/j.ijsolstr.2011.03.024

[5] Skrinar, M. "Elastic beam finite element with an arbitrary number of transverse cracks". *Finite Elements in Analysis and Design*, 45(3), 181–189. 2009.
https://doi.org/10.1016/j.finel.2008.09.003

[6] Skrinar, M., Pliberšek, T. "On the derivation of symbolic form of stiffness matrix and load vector of a beam with an arbitrary number of transverse cracks". *Computational Materials Science*, 52(1), pp. 253–260. 2012.
https://doi.org/10.1016/j.commatsci.2011.07.013

[7] Labib, A., Kennedy, D., Featherston C. A. "Free vibration analysis of beams and frames with multiple cracks for damage detection". *Journal of Sound and Vibration*, 333(20), pp. 4991–5003. 2014.
https://doi.org/10.1016/j.jsv.2014.05.015

[8] Bakhtiari-Nejad, F., Khorram, A., Rezaeian, M. "Analytical estimation of natural frequencies and mode shapes of a beam having two cracks". *International Journal of Mechanical Sciences*, 78, pp. 193–202. 2014.
https://doi.org/10.1016/j.ijmecsci.2013.10.007

[9] Labib, A., Kennedy, D., Featherston, C. A. "Crack localisation in frames using natural frequency degradations". *Computers and Structures*, 157, pp. 51–59. 2015.
https://doi.org/10.1016/j.compstruc.2015.05.001

[10] Khiem, N. T., Toan, L. K. "A novel method for crack detection in beam-like structures by measurements of natural frequencies". *Journal of Sound and Vibration*, 333(18), pp. 4084–4103. 2014.
https://doi.org/10.1016/j.jsv.2014.04.031

[11] Khiem, N. T., Tran, H. T. "A procedure for multiple crack identification in beam-like structures from natural vibration mode". *Journal of Vibration and Control*, 20(9), pp. 1417–1427. 2014.
https://doi.org/10.1177/1077546312470478

[12] Sung, S. H., Koo, K. Y., Jung, H. J. "Modal flexibility-based damage detection of cantilever beam-type structures using base line modification". *Journal of Sound and Vibration*, 333(18), pp. 4123–4138. 2014.
https://doi.org/10.1016/j.jsv.2014.04.056

[13] Cao, M., Radzieński, M. Xu, W., Ostachowicz W. "Identification of multiple damage in beams based on robust curvature mode shapes". *Mechanical Systems and Signal Processing*, 46, pp. 468–480. 2014.
https://doi.org/10.1016/j.ymssp.2014.01.004

[14] Gawande, S. H., More, R. R., "Effect of Notch Depth & Location on Modal Natural Frequency of Cantilever Beams". *Structures*, 8, pp. 121–129. 2016.
https://doi.org/10.1016/j.istruc.2016.09.003

[15] Skrinar, M. "Computational analysis of multi-stepped beams and beams with linearly-varying heights implementing closed-form finite element formulation for multi-cracked beam elements". *International Journal of Solids and Structures*, 50(14–15), pp. 2527–2541. 2013.
https://doi.org/10.1016/j.ijsolstr.2013.04.005

[16] Vestroni, F. Lecture notes from the course "Dynamical Inverse Problems: Theory and Application", Udine, Italy. 2009.